

Distribution of the magnetization reversal duration in subnanosecond spin-transfer switching

T. Devolder,¹ C. Chappert,¹ J. A. Katine,³ M. J. Carey,³ and K. Ito²

¹*Institut d'Electronique Fondamentale, CNRS UMR 8622, Université Paris Sud, Bât. 220, 91405 Orsay, France*

²*Hitachi Cambridge Laboratory, Hitachi Europe, Ltd., Cavendish Laboratory, Madingley Road, Cambridge CB3 0HE, United Kingdom*

³*Hitachi GST, San Jose Research Center, 650 Harry Road, San Jose, California 95120, USA*

(Received 4 September 2006; revised manuscript received 23 October 2006; published 1 February 2007)

We study the experimental distribution of switching times in spin-transfer switching induced by sub-ns current pulses in a pillar-shaped spin valve, whose free layer easy axis is parallel to the spin polarization of the current. The pulse durations leading to successful switching events follow a multiply stepped distribution. The step positions reflect the precessional nature of the switching. Modeling indicates that the switching proceeds through an integer number of gradually amplified precession cycles. This number is determined by the initial magnetization state. The switching probability distribution can be modeled considering the thermal variance of the initial magnetization orientation and by analyzing the occurrence of a vanishing total torque condition in the set possible magnetization trajectories. Modeling helps us to understand why switching cannot happen with a reproducible sub-ns duration when the free layer easy axis is parallel to the spin polarization of the current. To circumvent that problem, we propose to bias the spin valve with a hard axis field, which could provide an increased reproducibility of the switching duration.

DOI: 10.1103/PhysRevB.75.064402

PACS number(s): 75.60.Ej, 72.25.Pn, 75.70.-i

The spin-transfer effect¹ is the exchange of angular momentum between a spin-polarized electrical current and the magnetization of a nanomagnet. The spin-transfer results in torques that can be used to manipulate magnetic configurations with a sole current. When a spin-transfer torque (STT) is used in a magnetoresistive system, the current can play two roles, since the electrical resistance can be used to probe the configuration that the current manipulates. In recent years, STT has been achieved in a variety of systems, leading to new phenomena such as nonohmic behavior in metallic multilayers,² displacement of domain walls,³ generation of spin waves,⁴ and pumping of small⁵ or large⁶ amplitude steady state magnetization precessions.

STT can also simply switch the magnetization of a uniaxial nanomagnet,⁷ which is considered as a promising route for memory applications,⁸ since this type of switching has proven deep sub-ns potential.^{9,10} However, previous investigations have concluded that the reversal speed in the sub-ns regime has insufficient reproducibility. This has first been interpreted qualitatively as resulting from classical thermal fluctuations,¹¹ but reliable predictions are not yet available.

In this paper, we show experimentally that the sub-ns pulse durations leading to successful switching events are *discrete* quantities reflecting the precessional nature of magnetization dynamics, and the topological peculiarities in the set of possible magnetization trajectories. This tendency towards quantization of the switching times can be manipulated using a hard axis field to lift the near degeneracy between magnetic trajectories. We discuss these findings by taking into account the precessional dynamics, the STT, and the thermal effects in the macrospin approximation.

Our devices are spin valves of composition PtMn17.5/CoFe1.8/Ru0.8/CoFe2/Cu3.5/CoFe1/NiFe1.8 (thickness in nm), etched into elongated hexagons, whose major axis is parallel to the PtMn exchange pinning direction. We have investigated two sizes: $75 \times 150 \text{ nm}^2$ (category

A) and $75 \times 113 \text{ nm}^2$ (category B); they yield similar results. The devices are similar to those used in Ref. 12, except that here they are inserted in a high frequency layout, whose bandwidth has been checked to be greater than 50 GHz using vector network analyzer measurements. The static properties of our samples are described in detail elsewhere.¹³ For category B, the mean quasistatic parallel state to antiparallel state (P \rightarrow AP) and AP \rightarrow P switching currents are 3 mA (i.e., $1.1 \times 10^8 \text{ A/cm}^2$) and -1.1 mA (i.e., $-5.3 \times 10^7 \text{ A/cm}^2$), respectively.

The ends of the device coplanar stripes are contacted to the instruments by means of coplanar-coaxial transitions of bandwidth 40 GHz. The setup allows for the simultaneous application and measurement of three electrical currents I_{dc} , I_{ac} , and I_{pulse} in separate frequency domains. The dc current (I_{dc} , 0–20 mA) induces the quasistatic switching of the magnetization of the free layer using the spin-transfer effect. A small modulation current ($I_{ac} = 72 \mu\text{A rms}$, $f = 67 \text{ kHz}$) is superimposed to allow for the measurement of the resistance $R(t)$ with a lock-in amplifier and a time resolution of around 1 ms. These low frequency currents are routed in the device through the dc (inductive) port of a bias tee. The rf (capacitive) port of the bias tee is connected to a voltage pulse generator through a power divider. The second port of this power divider is connected to a 50 GHz oscilloscope, whose role is to check for bad (inductive) contacts between the DUT and microwave probes using time domain reflectometry.

Note that the high frequency part of the setup is carefully matched to 50 Ω characteristic impedance from one end of the circuit to the other, ensuring no spurious voltage wave reflection except at the resistive (13.4 Ω) pillar itself. The pulse quality has been checked carefully. The voltage pulse amplitude V_{pulse} provided by the pulse generator can thus reliably be translated in a current pulse I_{pulse} . The reported pulse durations are FWHM with rise times of 55 ps.

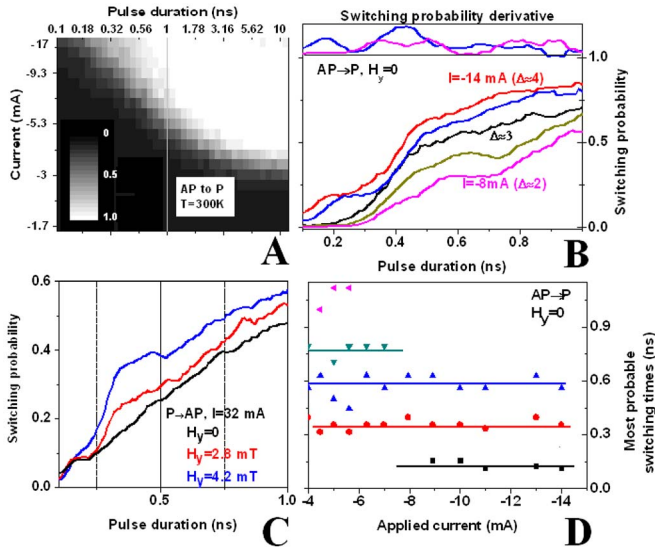


FIG. 1. (Color online) (a) Experimental AP to P switching probability versus current pulse magnitude and duration for a sample of category B. The gray level scales with the switching probability. (b) Horizontal cuts through Fig. 1(a): AP to P switching probability versus current pulse duration for -8 , -9 , -11 , -13 , and -14 mA current pulses. Top curves: distribution of the switching times for -13 mA (blue) and for -8 mA (magenta). (c) Experimental P to AP switching probability for a sample of category A submitted to 32 mA and static hard axis fields. (d) Applied current dependence of the most probable switching instants for AP to P switching in a sample of type B. The horizontal lines are guides to the eyes.

The measurement procedure for AP to P switching is the following. The sample is first prepared in the AP state by I_{dc} . R_{AP} is measured at remanence. The current pulse I_{pulse} is then applied and the resistance R' is determined after relaxation. A negative I_{dc} is then applied to ensure returns to the P state, and R_P is measured. The ratios $(R' - R_P)/(R_{AP} - R_P)$ are very near 1 or 0, indicating that the reversal is either complete or nonexistent. Each ratio is thus used to decide whether switching has occurred for a given current pulse duration and amplitude. The procedure is repeated 1000 times for each pulse amplitude/duration. To estimate the switching probability p versus I_{pulse} and τ_{pulse} , we measure n successful switching events out of $N=1000$ trials and say that $p \approx n/N$. Our finite number of trials results in a random Gaussian error $\Delta n/\langle n \rangle = \sqrt{p(1-p)}/N$. This error is at worst 1.6% when $p=50\%$. Note that our procedure does not involve averaging, since it examines the result of *each* switching trial. We are hence able to detect rare events, when any. This is complementary to time-domain averaging of the magnetization response using sampling techniques,^{14,15} that only record the *reproducible* part of a magnetic behavior, and that are therefore not appropriate to make precise evaluation of the switching reliability. We shall see that this difference in experimental methods is important since some specific initial conditions that occurring rarely, lead to a quasidivergence of the switching time.

In Fig. 1(a), we show the switching probability for the AP \rightarrow P transitions for a sample of category B and for pulse durations τ_{pulse} from 100 ps to 10 ns. Our results follow the

rule of thumb that the switching requires a pulse duration τ_{pulse} that scales with the inverse of the overdrive current $\Delta = (J_{applied} - J_{C0})/J_{C0} > 0$, where $J_{C0} \approx \alpha(\mu_0 M_{st}^2 t |e|)/(2\Pi\hbar) \approx 10^7$ A/cm² is the zero-temperature switching current, with t the free layer thickness, and Π the effective spin polarization. We write the applied current density as $J_{applied} = (\Delta + 1)J_{C0}$. The surface of the switching/no switching boundary indicates that the switching duration has a dispersion of about $\pm 30\%$.

In Fig. 1(b), we have zoomed on some horizontal cuts of Fig. 1(a): We set $J_{applied}$, vary the pulse duration τ_{pulse} by increments of 10 ps, and evaluate the resulting switching probability. The switching probability increases with τ_{pulse} , but this increase is not regular: Flat plateaus alternate with rounded steps [Fig. 1(b), bottom curves]. This behavior has been observed systematically for AP to P switching for $0.1 < \tau_{pulse} < 1.2$ ns. The steps are better revealed when looking at the differential switching probability density [Fig. 1(b), top curves]. The latter describes the probability that the reversal is induced at exactly the instant t (i.e., between time t and $t+dt$). It has a comblike structure, with most often two peaks at the we will hereafter quote as the *most probable switching instants*. The same trends have been observed for the reverse (i.e., P \rightarrow AP) transition, however with generally a fainter step-to-plateau contrast.

When we vary the current, we observe correlations between the *most probable switching instants* (i.e., step positions), indicating that they may reflect some periodicity in the magnetization reversal paths. We have thus gathered in Fig. 1(d) the most probable switching instants (i.e., the step positions) versus I_{pulse} for the AP \rightarrow P transition in samples B. The peak positions are labeled with symbols/colors according to their index. The shortest most probable switching instants (black squares) are grouped between pulse durations of 110 and 140 ps. They are observable only at currents higher than 9 mA. The second set of most probable switching instants (red circles) is grouped in the interval between 320 and 400 ps; these most probable switching instants were identified for all the studied applied currents [Fig. 1(b)]. Most of the third probable switching instants (blue triangles) arise between 560 and 630 ps.

Finally, we have performed additional measurements after applying a constant field H_y along the hard axis. A representative result is reported in Fig. 1(c); we display the switching probability distribution for the P to AP transition with a constant overdrive ($\Delta=6$) and a *variable hard axis applied field*. We can notice that for $H_y=0$, there is a single plateau at around $\tau_p=150$ ps, and switching probability curve is not that rich. When the field is raised to 2.8 mT (in this case, this corresponds to $H_k/4$), there appears a highly probable switching instant at 290 ps. When the field is further increased to 4.2 mT, the probability of switching at an instant $t=290$ ps is further reinforced, while the step at 150 ps disappears. More generally, we have observed that for P to AP as well as for AP to P transitions, adding a hard axis field reinforces or reveals some steps, while it make some other disappear.

In order to understand the origin of this comblike distribution of switching instant, we have performed extensive simulations. For this, we model the behavior of our well

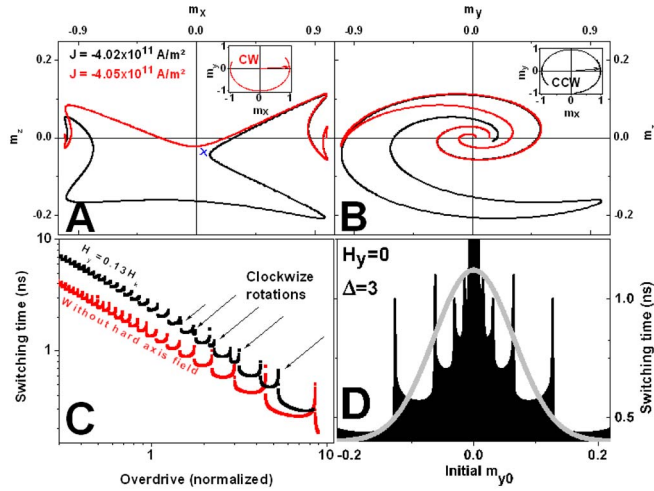


FIG. 2. (Color online) (a) (b) Calculated magnetization trajectories after the application of two current steps of slightly different amplitude, in zero applied field and with an initial magnetization following $m_{y0}=0.128$ and $m_{z0}=0$. Insets: In-plane projection of the magnetization trajectories, showing whether the switching happens by clockwise or counterclockwise rotation. (c) Calculated switching times versus overdrive current with initial magnetization following $m_{y0}=0.128$ and $m_{z0}=0$, and for $H_y=0$ or $\mu_0 H_y=0.128\mu_0 H_k=2.5$ mT. (d) Calculated switching time versus initial magnetization orientation in zero applied field and in a current corresponding to an overdrive parameter of 3. Gray curve: Boltzmann distribution of the initial magnetization.

characterized¹³ category B of samples using a thin macrospinning in the (xy) plane, having a magnetization $M_S=6.76 \times 10^5$ A/m ($\mu_0 M_S=0.85$ T), a thickness $t=2.8$ nm, a uniaxial anisotropy of $\mu_0 H_k=20$ mT along an easy axis (x) and a Gilbert damping parameter $\alpha=0.02$. The current carries a spin polarisation $\Pi=0.27$ along $(-x)$. We use a sinusoidal angular dependence of the STT, and the standard Landau-Lifshitz-Gilbert equation. Before the square current pulse is applied, the normalized magnetization is assumed to be $\mathbf{m}_0=\{m_{x0}, m_{y0}, 0\}$, i.e., in the film plane, near its equilibrium position.

Let us first consider the switching when there is no applied field ($H_y=0$). Representative reversal trajectories are displayed in Fig. 2(a) and 2(b) for $m_{y0}=0.128$ and two very near overdrive parameters of $\Delta=3.02$ (black) and $\Delta=3.05$ (red). The magnetization undergoes first an elliptical precession around its easy axis, with a growing precession amplitude. Depending on \mathbf{m}_0 and J_{applied} , the reversal proceeds through some finite number of half precession (NHP) cycles before magnetization overcomes the hard axis. We define NHP as the sum of the number of maxima and minima in the trace of $m_y(t)$, including that occurring when $m_x=0$. This definition of NHP is straightforward when counting the number of turn in Fig. 2(b) before the cusp in the $\{m_y, m_z\}$ trajectories. NHP is odd (even) when the magnetization switching occurs by a clockwise (counterclockwise) rotation in the $\{m_x, m_y\}$ plane [see insets in Fig. 1(a) and 1(b)]. We write CW (CCW) for clockwise (respectively counterclockwise) rotations. After having overcome the hard axis, the magneti-

zation finally relaxes to the reverse easy axis position ($m_x=-1$) following a heavily damped precessional trajectory.

While NHP is 3 for $\Delta=3.05$, a marginally smaller overdrive $\Delta=3.02$ leads to NHP=4. In between $3.02 < \Delta < 3.05$, there is a remarkable current density $J_{\text{max jitter}}$. The reason why we index this current density as the “maximum jitter” current density will appear clearly later in the discussion. For $J_{\text{applied}}=J_{\text{max jitter}}$, the magnetization passes at a specific orientation [cross in Fig. 2(a)] with $m_x=0$ where the demagnetizing and the spin torques cancel each other; the magnetization feels a *vanishing total torque*, and a perturbation is needed to either switch immediately or perform another half precession cycle before indeed switching. At this specific magnetization orientation, the magnetization $\{m_x, m_y, m_z\}$ follows $m_x=0$ and

$$J_{\text{max jitter}} = \frac{m_z 2\mu_0 M_S^2 t |e|}{m_y \Pi \hbar}. \quad (1)$$

The latter expression can be easily found by setting $m_x=0$, $m_y \approx \pm 1$ and balancing the demagnetization field $M_S \cdot m_z \cdot \mathbf{e}_z$ with the spin torque expressed as a field, i.e., $(2\mu_0 \Pi J / \hbar t M_S |e|) \mathbf{p} \times \mathbf{m}$. Since $m_x=0$, there is no anisotropy field acting on the magnetization at that position. Note that since in practice the applied current satisfies $\Delta \alpha \ll 2$, there exists two initial conditions leading magnetization trajectories passing through magnetization orientations that satisfy Eq. (1).

The happening of a vanishing total torque yields two important consequences for the switching duration $\tau_{m_x=0}$ and its repeatability. For stochastic initial conditions, the possibility of satisfying Eq. (1) may add an incremental *jitter* of exactly half a precession period to the overall switching time. This results in a steplike dependence of $\tau_{m_x=0}$ versus current at given m_{y0} [see Fig. 2(c)], or to a steplike dependence of $\tau_{m_x=0}$ versus m_{y0} [see Fig. 2(d)] at given current. In addition, when approaching a vanishing total torque magnetization orientation [Eq. (1)], the reversal time $\tau_{m_x=0}$ diverges [see Figs. 2(c) and 2(d)]. In Fig. 3(a), we report the switching times versus both the initial magnetization orientation m_{y0} and the overdrive current, in zero field. The divergence of the switching time for initial magnetization along the easy axis ($m_{x0}=1$) appears as a horizontal line. The conditions for vanishing total torques appear as curved contours, separating switching regions with differing NHP.

Due to the finite temperature, each switching test encounters a different initial condition $\{m_{x0}, m_{y0}, m_{z0}\}$, with an orientation randomly distributed near the easy axis. We model this distribution using Boltzmann statistics. The distribution of the in-plane projection of the magnetization [Fig. 2(d)] has a width of $m_{y0}^{\text{rms}} = \sqrt{(kT)/(\mu_0 H_k M_S V)}$. This width is 0.13 at $T=300$ K. It is sketched as the vertical segment in Fig. 3(a). Note that the initial magnetization has in principle also a fluctuating out-of-plane component $m_{z0}^{\text{rms}} = \sqrt{(kT)/(\mu_0 M_S^2 V)}$. That out-of-plane fluctuation is typically seven times lower than the in-plane fluctuation. Since we aim at qualitative understanding of our experimental findings, we will only consider the statistical fluctuation of m_{y0} and we will disregard that of m_{z0} in our forthcoming calculations.

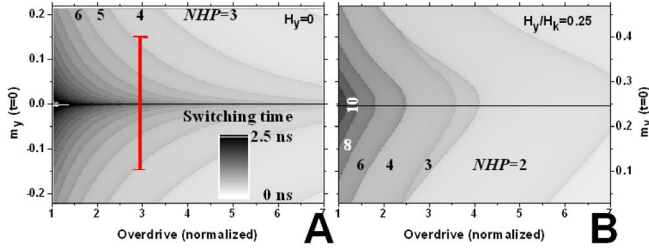


FIG. 3. (Color online) Calculated switching time versus initial magnetization orientation and overdrive current, (a) in zero applied field. The vertical segment indicates the width of the thermal distribution of initial states. (b) An applied field of $H_y=0.13H_k$, i.e., $\mu_0H_y=2.5$ mT. The numbers superimposed on the graph indicate the number of half precession cycles needed for magnetization reversal.

For statistical m_{y0} with a current $\Delta=3$, a majority of switching events requires NHP to be 4 or 5 while a few events will require more NHP [Fig. 3(a)]. This will appear in the probability of successful switching with a given overdrive, as calculated in Fig. 4(a) for overdrives ranging from 3 to 7.

To perform these calculations, we first assume some fixed overdrive current. We then consider a set of initial states regularly spaced between $-1 < m_{y0} < 1$, with $m_{z0}=0$, and calculate the switching time for each initial state (Fig. 3). We then assign each obtained switching time a probability according to the statistical occupancy of the initial state according to a Boltzmann distribution [Fig. 2(d), blue curve], and construct an histogram of the weighted switching times. Integration of this weighted histogram provides the distribution of switching probability versus pulse duration for the initially chosen overdrive.

These calculated distributions of switching times [Fig. 4(a)] compares qualitatively well with experiments [Fig. 1(b)], despite the fact that no fitting procedure has been attempted and that we have disregarded any possible out-of-plane component in the distribution of possible initial magnetizations. The model reproduces the overall behavior that the switching time shall increase steplike with the pulse duration, and that the position of the steps do not depend much on the applied current. More precisely, the calculated most probable switching instants slightly shift to small durations when the overdrive increases [see dotted lines in Fig. 4(a)].

Almost quantitative agreement is obtained between the experimental most probable switching instants [Fig. 1(d)] and some step positions (dotted lines) in Fig. 4(a). However, this agreement is probably fortuitous, since the experimental shortest switching times at 140 ps pulse duration cannot be reproduced by our model. The steps are steeper in the calculation than in the experimental results, indicating that although our model captures the essential physics, it neglects some effects that decrease the coherency of the magnetization trajectories. In our model, thermal fluctuations are only partially taken into account by the statistics of the possible initial states, but are neglected during reversal path. We conjecture that thermal noise during the reversal path, by randomly slowing or increasing the rate of growth of the precession amplitude will result in a softening of the steps in the

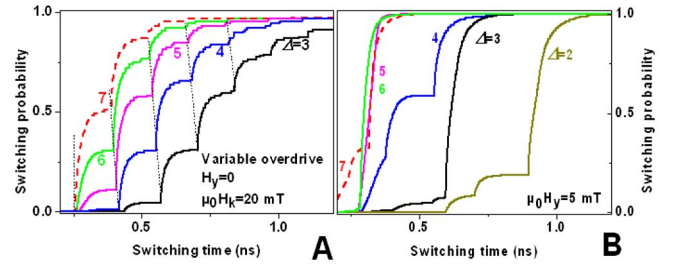


FIG. 4. (Color online) Calculated switching probabilities versus pulsed current duration at temperatures for several overdrive currents (a) in zero applied field. The near vertical dotted lines correspond to the most probable switching instants (b) in a hard axis applied field of $H_y=0.25H_k$.

switching probability distribution. We also have neglected here the effect of the ampere field, according to previous work¹¹ that concluded that its role is secondary at room temperature for the AP to P transition. In a few micromagnetic simulations, we have taken into the ampere field and the temperature in full micromagnetics formalism following the methods described in Ref. 16. Computational time constraints restrict these simulations to few snapshots in the parameter space $\{\tau_{\text{pulse}}, I_{\text{pulse}}\}$, but they confirm the prediction of steps in the switching probability distribution versus pulse duration.¹⁷ To summarize, our most salient result is that when the magnetization of the reference layer is parallel to the easy axis of the free layer, sub-ns switching is possible, but the switching time jitters by multiple increments of a half precession period. Both from the experiment and from the modeling, we can conclude that there is no overdrive current that can make the switching time reproducible at room temperature. We shall see that applying a hard axis field is one way to improve the overall reproducibility.

We thus now simulate the effect of a hard axis field. The initial magnetization orientation is chosen near its equilibrium $\langle m_{y0} \rangle = H_y/H_k$, with a variance of the in-plane component still assumed to follow Boltzmann statistics. As formerly done in the zero-field case, we still assume that the initial magnetization lies strictly in the film plane. The first important difference with the zero-field case is that when there is an applied field, the spin-torque gets finite as soon as the current is applied. Even when the magnetization is strictly at equilibrium with the applied field, the spin torque has a finite out-of-the-film-plane component that is $\Pi J \hbar m_{y0} / (2 \mu_0 M_{st} |e|)$. Hence, in contrast to the zero field case, there is *no divergence* of the switching speed when the magnetization is exactly along its in-field equilibrium position [compare Figs. 3(a) and 3(b)]. This removal of divergence is a clear benefit of applying a hard axis field.

However, there is another important change induced by the applied field. Without applied fields, switching by CW rotation (odd NHP) or CCW rotation (even NHP) takes place with comparable probabilities. This does not hold when $H_y \neq 0$: Small overdrives only lead CCW rotations, and the reversal proceeds by passing near the hard direction favored by the field, i.e., near $m_y=1$ if $H_y > 0$. This is illustrated in Fig. 3(b), which summarizes the switching times versus m_{y0} and Δ , when a static hard axis field $H_y=0.25H_k$ is applied.

The crossing of a vanishing total torque contours at overdrives $\Delta < 3$ corresponds to changes in NHP by *increments of two units* and the switching is always of CCW nature. Only at larger overdrives, some initial conditions m_{y0} can lead to CW rotations, and the crossings of a vanishing total torque contours change the NHP by increments of one unit.

As done previously in zero applied field, we can mimic a thermal distribution of initial states by affecting to each initial state an occupancy factor according to Boltzmann statistics. We then calculate for $H_y \neq 0$ the switching probability versus pulse durations [Fig. 4(b)] taking into account the set of switching times resulting from each considered initial state, weighted by its thermal occupancy factor. We still consider only initial states whose magnetization are strictly in the sample plane. At overdrives $\Delta \leq 4$, the various possible initial magnetization orientations can lead to several NHP values [see Fig. 3(b)], such that the switching probability is multiply stepped versus the pulse duration [Fig. 4(b)]. However, since the NHP can only take *even* values at overdrives $\Delta \leq 4$, the number of steps is typically *twice less* than in the zero-field case, and their height is enhanced by the field [Fig. 4(a)]. This correlates well with our experimental results.

Interestingly, at overdrives $\Delta = 5$ and 6, almost any initial magnetization within the Boltzmann distribution leads to a reversal taking NHP=2. The reversal duration is thus expected to be very reproducible from one switching event to the next [Fig. 4(b)]; this is interesting since this could be used to render the switching time more reproducible.

Attempting to further accelerate the switching by increasing the overdrive current to 7 is predicted to be detrimental

to the reproducibility of the switching duration, because it introduces two drawbacks. It first triggers some faster reversal events requiring one less precession cycle. The switching probability versus pulse duration at $\Delta = 7$ has then a foot near fast pulse durations. As an additional drawback, raising the overdrive from 6 to 7 also makes possible a few trajectories passing near or through a zero torque position, which generates consequently a small number of very slow switching events: the switching probability versus pulse duration at $\Delta = 7$ has then a slow saturation [Fig. 4(b)] at pulse durations above 300 ps.

In summary, we have studied sub-ns spin-transfer switching. The current pulse durations leading to switching follow a steplike distribution. Modeling indicates that depending on the initial magnetization and the current amplitude, specific vanishing total torque magnetization position in the possible magnetization trajectories make the switching duration susceptible to jitter by increments of the half precession period. The nature of these vanishing torque positions also implies that the reversal time diverges for a few initial conditions. All together, it seems impossible to get magnetic field-free, reproducible current-induced sub-ns switching times, when using a system with a free layer easy axis that is parallel to the reference layer magnetization. Modeling in the macrospin approximation indicates that this problem may be solved by the application of a hard axis field. We predict that, at large overdrives, this hard axis applied field could even suppress the vanishing torque positions, allowing a satisfactory reproducibility of the switching time.

¹J. Slonczewski, J. Magn. Magn. Mater. **159**, 1 (1996).

²M. Tsoi, A. G. M. Jansen, J. Bass, W. C. Chiang, M. Seck, V. Tsoi, and P. Wyder, Phys. Rev. Lett. **80**, 4281 (1998).

³E. Saitoh, H. Miyajima, T. Yamaoka, and G. Tatara, Nature (London) **432**, 2003 (2004).

⁴B. Özyilmaz, A. D. Kent, J. Z. Sun, M. J. Rooks, and R. H. Koch, Phys. Rev. Lett. **93**, 176604 (2004).

⁵T. Devolder, P. Crozat, C. Chappert, J. Miltat, A. Tulapurkar, Y. Suzuki, and K. Yagami, Phys. Rev. B **71**, 184401 (2005).

⁶S. I. Kiselev, J. C. Sankey, I. N. Krivorotov, N. C. Emley, R. J. Schoelkopf, R. A. Buhrman, and D. C. Ralph, Nature (London) **425**, 380 (2003).

⁷J. A. Katine, F. J. Albert, and R. A. Buhrman, Appl. Phys. Lett. **77**, 3809 (2000); J. A. Katine, F. J. Albert, R. A. Buhrman, E. B. Myers, and D. C. Ralph, Phys. Rev. Lett. **84**, 3149 (2000).

⁸M. Hosomi *et al.*. A Novel Nonvolatile Memory with Spin Torque Transfer Magnetization Switching: Spin-RAM, *Proceedings of IEDM Conference*, 2005 (unpublished).

⁹A. A. Tulapurkar, T. Devolder, K. Yagami, P. Crozat, C. Chappert,

A. Fukushima, and Y. Suzuki, Appl. Phys. Lett. **85**, 5358 (2004).

¹⁰T. Devolder, C. Chappert, P. Crozat, A. Tulapurkar, Y. Suzuki, J. Miltat, and K. Yagami, Appl. Phys. Lett. **86**, 062505 (2005).

¹¹T. Devolder, A. Tulapurkar, Y. Suzuki, C. Chappert, P. Crozat, and K. Yagami, J. Appl. Phys. **98**, 053904-1 (2005).

¹²D. Lacour, J. A. Katine, N. Smith, M. J. Carey, and J. R. Childress, Appl. Phys. Lett. **85**, 4681 (2004).

¹³T. Devolder, K. Ito, J. A. Katine, P. Crozat, J.-V. Kim, and C. Chappert, Appl. Phys. Lett. **88**, 152502 (2006).

¹⁴N. C. Emley, I. N. Krivorotov, O. Ozatay, A. G. F. Garcia, J. C. Sankey, D. C. Ralph, and R. A. Buhrman, Phys. Rev. Lett. **96**, 247204 (2006).

¹⁵Y. Acremann, J. P. Strachan, V. Chembrolu, S. D. Andrews, T. Tylliszczak, J. A. Katine, M. J. Carey, B. M. Clemens, H. C. Siegmann, and J. Stohr, Phys. Rev. Lett. **96**, 217202 (2006).

¹⁶K. Ito, T. Devolder, C. Chappert, M. Carey, and J. Katine, J. Appl. Phys. **99**, 08G519 (2006).

¹⁷K. Ito (private communication).